The Discovery and Characterization of an Ultracompact Hot Subdwarf and Brown Dwarf Binary System

by

Lisa Nicole Blomberg

Submitted to the Department of Physics
in partial fulfillment of the requirements for the degree of
Bachelor of Science in Physics
at the
MASSACHUSETTS INSTITUTE OF TECHNOLOGY
June 2023

Author .....
Department of Physics
May 12th, 2023

Certified by .....
Kevin B. Burdge
Pappalardo Fellow in Physics
Thesis Supervisor

Certified by .....
Deepto Chakrabarty
Department Head, Professor
Thesis Supervisor

Accepted by .....
Lindley Winslow
Associate Department Head of Physics, Associate Professor

The Discovery and Characterization of an Ultracompact Hot Subdwarf and Brown Dwarf Binary System

by

Lisa Nicole Blomberg

Submitted to the Department of Physics
on May 12th, 2023, in partial fulfillment of the
requirements for the degree of
Bachelor of Science in Physics

Abstract

Stellar binary systems are astronomical objects made of two stars gravitationally bound to each other. In some of these systems, the stars are so close that they interact with each other and affect the formation and evolution of one another. As a result, understanding these objects can provide insight into various stellar processes and astrophysical phenomena. In my project, I focused on studying a type of ultra-compact binary system called an HW Vir class binary – which is comprised of a hot sub dwarf and a brown dwarf. Because HW Vir systems can only be produced through the common envelope effect (CEE), understanding their physical parameters allows us to better understand the limitations of the CEE. For example, by studying binaries with the lowest mass companion that have survived the CEE, it allows us to draw conclusions about the lower bound on the companion mass that is able to survive envelope ejection. In my thesis, I outline the methods I used to search for these binary systems and model the lightcurve of ZTFJ2203+4824, a 78-minute orbital period HW Vir class binary that I discovered.

Thesis Supervisor: Kevin B. Burdge
Title: Pappalardo Fellow in Physics

Thesis Supervisor: Deepto Chakrabarty
Title: Department Head, Professor

Acknowledgments

First of all, I would like to thank Dr. Kevin Burdge who has mentored me over the past 15 months as a UROP advisor and as my thesis advisor. He has been encouraging and supportive at all times and most importantly has shown me how exciting research is. I would also like to thank Prof. Peter Fisher, who I met in my first year advising seminar, who has gone above and beyond as an academic advisor. Finally, I could not write an acknowledgement without addressing my family. I would not me where I am today if not for their continuous support and unconditional love.

Contents

List of Figures

List of Tables

Chapter 1

Introduction

When we look at the night sky, we see thousands of stars with our naked eye, and in addition to that, there are hundreds of billions more stars in our own Galaxy that we cannot see unaided. There are approximately 10^{23} stars in our universe and $\sim 10^{11}$ stars in the Milky Way. Each star formed and evolved in its own way and has a story of its own. As astrophysicists and astronomers, it is our goal to understand these stories and uncover the underlying physics of these processes. There are many avenues in which physicists approach this seemingly daunting task of understanding the nature of our universe outside the scope of our reach. One way physicists approach this subject is by studying the interaction of astronomical objects, and binary systems are a great tool for this. Because the two objects in a binary system are in proximity of each other, they allow researchers to observe and better understand how two astronomical objects interact with each other, and how those interactions affect the formation and evolution of stars.

The goal of this project was to search for and study eclipsing binary star systems to better understand various stellar formation and evolutionary processes. In particular, I focused on searching for short-period HW Vir class systems, and after discovering one, ZTFJ2203+4824, I focused on modeling its lightcurve. An HW Vir is a binary system comprised of a hot subdwarf with a hydrogen-rich companion. In Chapter 2, I will discuss the dataset and the instrumentation that I used in my analysis: the Zwicky Transient Facility (ZTF) and Caltech HIgh-speed Multi-color camERA

(CHIMERA) photometer on the 200 inch Hale telescope at the Palomar Observatory. In Chapter 3, I will discuss the properties and significance of studying HW Vir class binary systems with an orbital period under 80 minutes. Then in Chapters 4 and 5, I will discuss the methods of period searching that I employed to search for these HW Vir class binary systems and the fitting methods that I used to model the lightcurves to determine the physical parameters of these systems. Finally, we will conclude in Chapter 6 with a discussion of the results and areas of further research.

1.1 Stars

Astronomers categorize stars based on what elements are fusing in the stars' cores, which is closely related to their evolutionary stage. Generally, stars are categorized into three groups: the main sequence stars, the red giants, and the white dwarfs. We determine which group a star belongs in by studying its position on a Hertzsprung–Russell diagram (HR diagram). The HR diagram is depicted in one of two ways; it either plots the color (i.e., the temperature) of the star against its absolute brightness (i.e., luminosity), or the spectral class of the star (i.e., type O, B, A, F, etc.) against a measure of its brightness (i.e, the absolute magnitude). Note that temperature and color are used synonymously here because the color of a star is directly related to its surface temperature. This is because a star is approximated as a blackbody where the temperature of the object is directly proportional to the wavelength of the electromagnetic radiation the object is emitting. The relation is given by Wien's Displacement Law:

$$\lambda T = 2.898 \times 1010^{-3}\text{mK} \tag{1.1}$$

where λ is the peak wavelength (meters) of the black-body spectrum and T is the surface temperature (Kelvin) of the object. See Figure 1-1 for an example of an HR diagram.

The cluster of stars that run diagonally from the left-top (hot-luminous) of the plot, through the center, to the right-bottom (cold-faint) of the plot makes up the

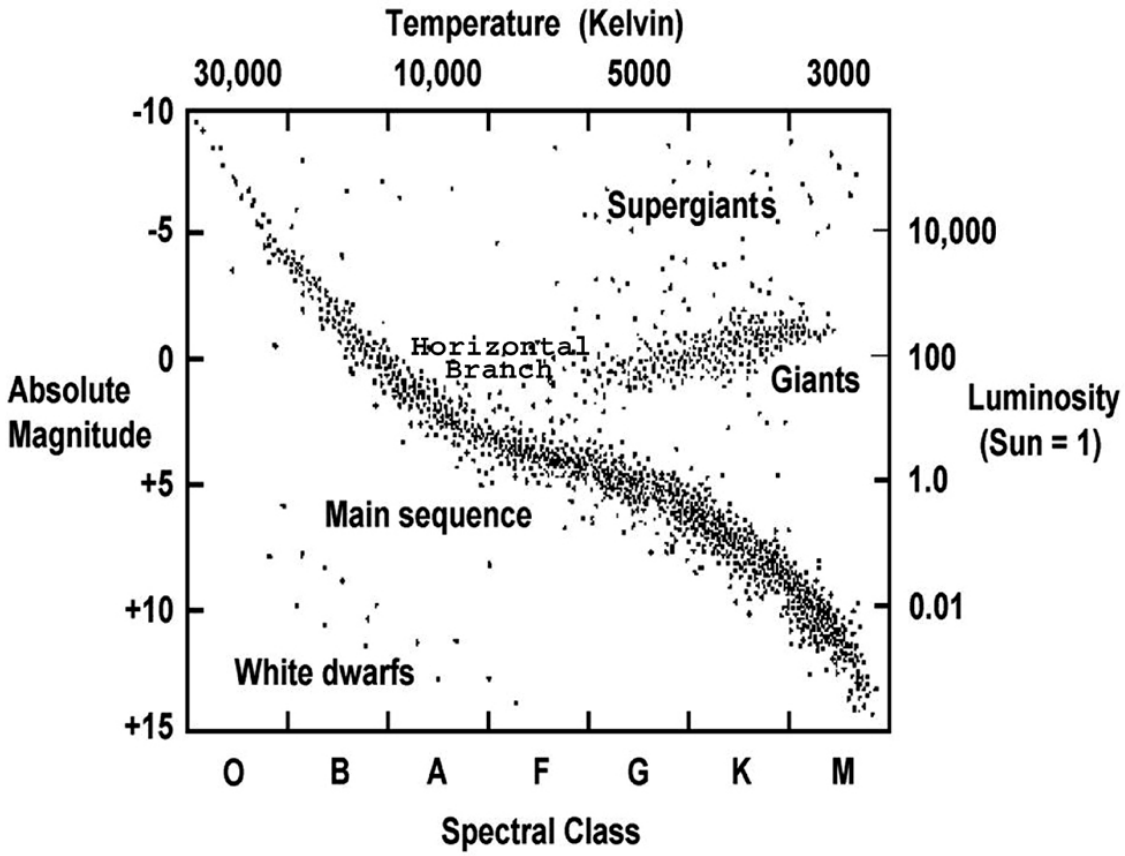

Figure 1-1: A HR diagram with its various branches labeled [1]. Along the center of the plot (from the top-left to the bottom-right corner) are the main sequence stars. As these stars evolve and no longer is able to fuse hydrogen in their cores, they become red giant stars which are located in the top-right corner (labeled as the supergiants and giants here). Finally, at the end of the star's life cycle, they evolve into white dwarfs which are located in the bottom-left corner of the HR diagram. Note that there are several conventions for the axis of HR diagrams, as marked on this plot: spectral class vs. absolute magnitude or temperature vs. luminosity.

main sequence branch. The stars in this region have hydrogen-fusing cores and approximately 90% of all stars lie in this region. When a main sequence star fuses through all of the hydrogen in its core, it starts to fuse hydrogen in its shell around the core. As this process takes place, the stars transition into red giants which are located along the *red giant branch* in the right-top (cold-luminous) corner of the plot. In Figure 1-1 the "supergiants" and the "giants" together make up the red giant branch. These stars tend to be larger than the main sequence stars, as the name suggests, and as predicted by their high luminosities but low temperatures. Once a red giant

is done fusing its heavier elements and no longer is able to continue fusing, the star leaves it core behind becoming a *white dwarf*. These stars lie in the left-bottom (hot-faint) region of the HR diagram, and have a relatively small size compared to the main sequence stars and the red giants.

1.2 Binary Systems

When two astronomical objects are gravitationally bound and orbit a common barycenter, they are referred to as a *binary system*. These systems can be comprised of a variety of different astronomical objects: stars, planets, black holes, etc. Due to the nature of these systems, the objects in a binary often interact with one another and plays a role in the evolution of its companion and of the system as a whole. For this project, I specifically studied stellar binary systems (i.e., binary systems comprised of two stellar objects) which are observable in the visible light range. Later in Chapter 3, I will further discuss the details of the HW Vir class binary systems which I choose to investigate for this project; but for now, let's discuss them in a more general sense.

1.2.1 Eclipsing Binary Systems

Eclipsing binary systems are a subset of binary systems with inclination angles ranging between approximately 70 to 90 degrees. This high inclination results in an observation of an eclipse of the system. This means that we see object 1 passing in front of object 2 at the beginning of a cycle, then at approximately mid-cycle, we see object 2 passing in front of object 1; finally, we return to the initial configuration where object 1 is in front of object 2 when the system has completed a full orbit. See Figure 1-2 for a schematic of a fully eclipsing system. The edge-on view is what the detector observes, and the face-on view is given for clarity. Note that this schematic is of a completely eclipsing system because from the observer's line of sight, the objects fully align with each other during the eclipse (i.e., when the blue object is in front, it will completely cover the pink object).

These systems are of great interest in astronomical studies for several reasons.

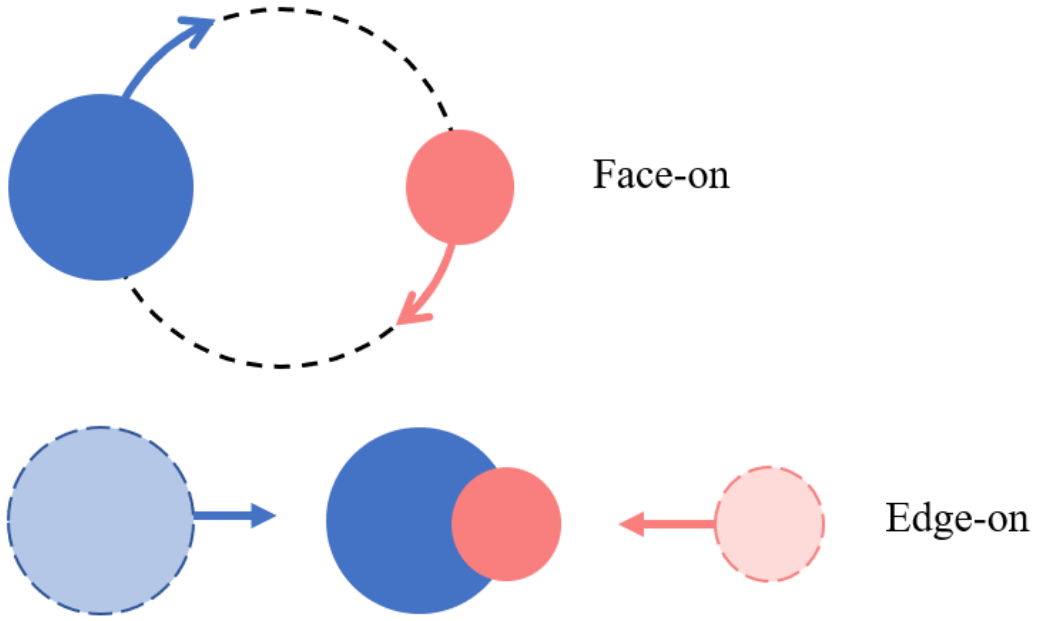

Figure 1-2: Schematic of a totally eclipsing binary system. If we are observing an eclipse face-on (top), the objects will never pass in front of each other. However, for an edge-on case (bottom), during a full orbit, each of the objects will pass in front of the other resulting in a total of two eclipses during each orbit. These are the two extreme cases where the inclination is 0 degrees (i.e., face-on) and 90 degrees (i.e., edge-on); often, the system is observed at some intermediate angle in between the above two cases.

First, the eclipsing nature allows us to study the properties of each of the stars separately during the two eclipses. When we see a binary from an edge-on view, as seen in Figure 1-2, we see eclipses in their lightcurves. We can use the information about the change in flux right before and after the eclipse to model certain physical parameters of the systems, such as the stars' radii and brightness ratio. We will further explore this in Chapters 1.3 and 5, in our discussion of light curves and modeling methods.

1.3 Light Curves

One common method for the study of stellar objects is through photometry (i.e., studying variations in electromagnetic flux over time). This type of data can be

represented in a lightcurve as show in Figure 1-3.

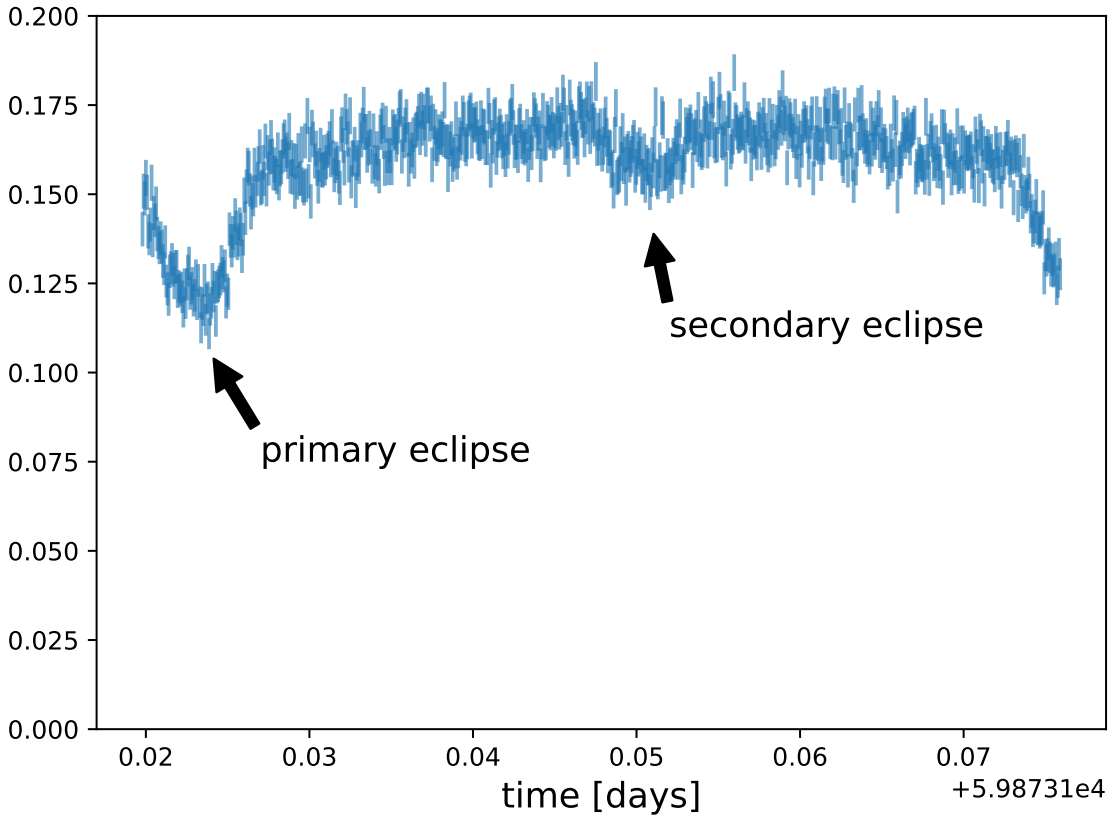

Figure 1-3: An example lightcurve; the lightcurve of ZTFJ2203+4824 (RA = 330.82, Dec = 48.40) from the g band photometric data from CHIMERA. The primary and secondary eclipses are as labeled above.

There are a few key features for lightcurves of eclipsing binary systems that are important to note. As we see labeled in Figure 1-3, there are two minima in the lightcurve, which mark the two different eclipses: the primary and the secondary eclipse. Eclipses take place when the binary is in *conjunction*– that is when both of the objects in the binary lie on our line of sight. The *primary eclipse* is observed when the more luminous star is eclipsed by the other star (i.e., when the fainter star is in front of the brighter star); this happens when the system is at its *superior conjunction*. On the other hand, the *secondary eclipse* is observed when the less luminous star is eclipsed by the more luminous star; this happens when the system is at its *inferior conjunction*. During the eclipsing regions, the light from one of the stars is blocked by

the other resulting in a decrease of the apparent photon flux to an observer viewing the system edge-on. Note that depending on the brightness ratio and the relative size of the stars, the secondary eclipse is not always readily apparent.

Further, the shape of the eclipsing regions allows us to better understand various properties of the binary system. Lightcurve models often take into account four parameters: the depth of the primary eclipse F_1 and the depth of the secondary eclipse F_2, and the start and end times of the egress ϕ_3 and ϕ_4, respectively. Let's take a look at a few examples of how these measurements relate to the physical parameters of a binary system to appreciate the wealth of information a lightcurve contains [4]. For example, the timing of the ingress (the downward-sloping region before the eclipse) and the egress (the upward-sloping region right after the eclipse) gives us information about the radii of the stars and their relative distances from each other:

$$\sin^2(i)\sin^2(2\pi\phi_3) + \cos^2(i) = \left(\frac{R_2}{a} - \frac{R_1}{a}\right)^2 \tag{1.2}$$

$$\sin^2(i)\sin^2(2\pi\phi_4) + \cos^2(i) = \left(\frac{R_1}{a} + \frac{R_2}{a}\right)^2 \tag{1.3}$$

where i is the inclination, a is the semi-major axis, and R_1 and R_2 are the radii of each of the stars in the binary system. Simply from the time stamp of the egress and the inclination, we are able to extract useful information about the relative size scale of the system (e.g., R_1/a and R_2/a). In addition, the shape and the depth of the eclipsing regions can provide information to us about the inclination and the brightness ratio. The shape of the lightcurve at the minimum (i.e., during the eclipse) tells us about the inclination of the binary; in other words, how the orbital plane of the binary is oriented with respect to our line of sight. If the system undergoes "total" eclipse (i.e., the stars align right in front of each other in our line of sight), we find that the eclipse will have a flat bottom. This is because during a total eclipse, one of the stars is completely covered by its companion and we only measure the photon flux from one of the objects. When we are only observing the flux from one of the stars, there is no change in flux and results in a constant (i.e., flat) bottom eclipsing region. We can also learn about the brightness ratio J of the two stars based on the

relative depths of the eclipsing regions:

$$J = \frac{1 - F_1}{1 - F_2}. \tag{1.4}$$

Even though lightcurves provide a wealth of information, not all physical parameters of these systems can be determined by their lightcurve alone. Measuring physical parameters such as the masses of the stars or the semi-major axis requires an analysis of their spectroscopic data in addition to the photometric data. For this project I focused on determining the physical parameters which can be determined by the lightcurve alone.

Another important characteristic of lightcurves of eclipsing binary systems are their periodicities. As discussed in Chapter 1.2, the two stars in a binary system are orbiting around each other with some given period. This means that for every cycle, we observe the sane lightcurve pattern with a primary and a secondary eclipse. The above example (Figure 1-3) only shows one orbital cycle, but if we have data from a longer observation, we would see the primary and secondary eclipse to repeat itself every cycle.

Finally, note the behavior in the out-of-eclipse regions. Different types of binary systems can exhibit different behaviors in these regions such as a sinusoidal pattern. These patterns are again linked to certain properties of the binary system. Although we will not go into details here, we will further discuss these effects for HW Vir class binaries later in Chapter 3.2.

Chapter 2

Data and Instrumentation

As briefly mentioned in Chapter 1, I used photometric datasets to search for and model binary systems. Specifically, I used the public data from the Zwicky Transient Facility (ZTF) to search for short-period eclipsing binary systems and requested to collect follow-up data on the target of interest on the high-speed imager, Caltech HIgh-speed Multi-color camERA (CHIMERA), on the Hale telescope at Palomar observatory. In this chapter, I will provide an overview of the ZTF survey and CHIMERA.

2.1 Open Data-Sources

There are several publically available astronomical photometric datasets, including data from the Transient Exoplanet Survey Satellite (TESS) [5] and the Zwicky Transient Facility (ZTF) [6]. Although often the data from large scale surveys and missions are lower resolution than those that you would be able to collect from doing a follow-up study on telescopes, they provide a good ground for large-scale studies and data mining for certain astronomical objects. For my research, I used the public data from ZTF to search for short-period binary systems.

2.1.1 Zwicky Transient Facility: ZTF

The Zwicky Transient Facility (ZTF) [6][2] is installed on the 48 inch Samuel Oschin Telescope (Schmidt-type), which is located at the Palomar observatory in the Palomar Mountain (north San Diego County, California). Figure 2-1 is a picture of ZTF at the Palomar observatory. 50 % of its time is used to complete a survey of the entire Northern sky every 2 days in both the r and g band. The data is then processed and released to the public regularly.

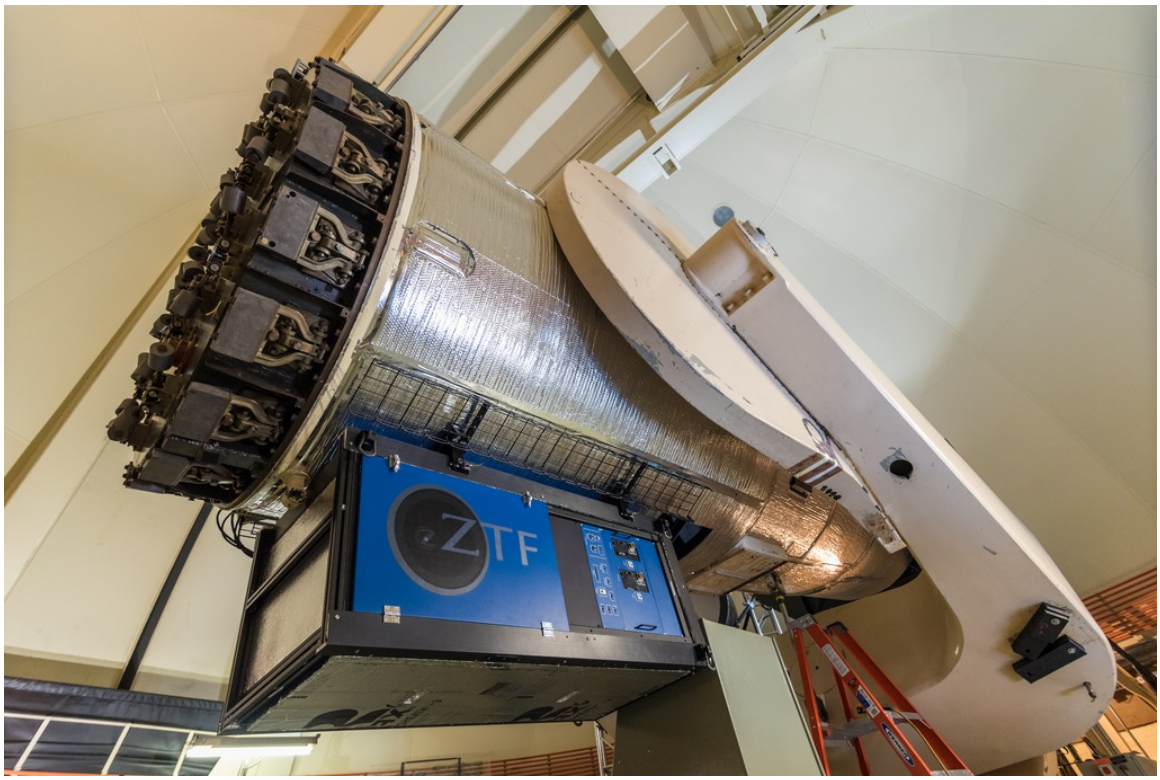

Figure 2-1: A picture of ZTF at the Palomar observatory [2]. I used the images taken with ZTF to discover ZTFJ2203+4824, the 78-minute orbital period binary studied in this thesis.

ZTF has a CCD camera which allows it to collect time-domain photometric data. Because ZTF is ground-based, it is able to collect much more sensitive data compared to other space-based missions. This is because space-based missions tend to be limited in their aperture, due to the high cost of sending large mirrors in to space. As a result, data from space-based surveys like TESS tend to have higher precision but lower sensitivity than ground-based surveys like ZTF. The higher sensitivity of ZTF allows

for higher resolution lightcurves which makes it more ideal – than a space-based survey such as TESS – for my project. However, one limitation of the ground-based survey is the limitation in the depth of observation due to the effects of the atmosphere, which resulted in a limitation in the scope of distance and luminosity of the stars that I could study.

2.2 Caltech HIgh-speed Multi-color camERA: CHIMERA

Although ZTF and other public datasets are useful for detecting binary systems, the data is often not sensitive enough for detailed modeling. Other instruments such as the Caltech HIgh-speed Multi-color camERA (CHIMERA) [7][3] can be used for these purposes. CHIMERA is a high-speed, two-color, wide-field photometer that is located on the Palomar telescope in California (at the same observatory as ZTF). One of its main missions is to study short periodic objects and is often used for collecting follow-up data on targets of interest that were detected by ZTF. See Figure 2-2 for a picture of the detector.

For this project, I requested to collect follow-up data for ZTFJ2203+4824 on CHIMERA. Through Dr. Kevin Burdge's connections to the California Institute of Technology, which operates the Hale telescope and the instrument CHIMERA, I acquired higher frame rate g and r band photometery for ZTFJ2203+4824.

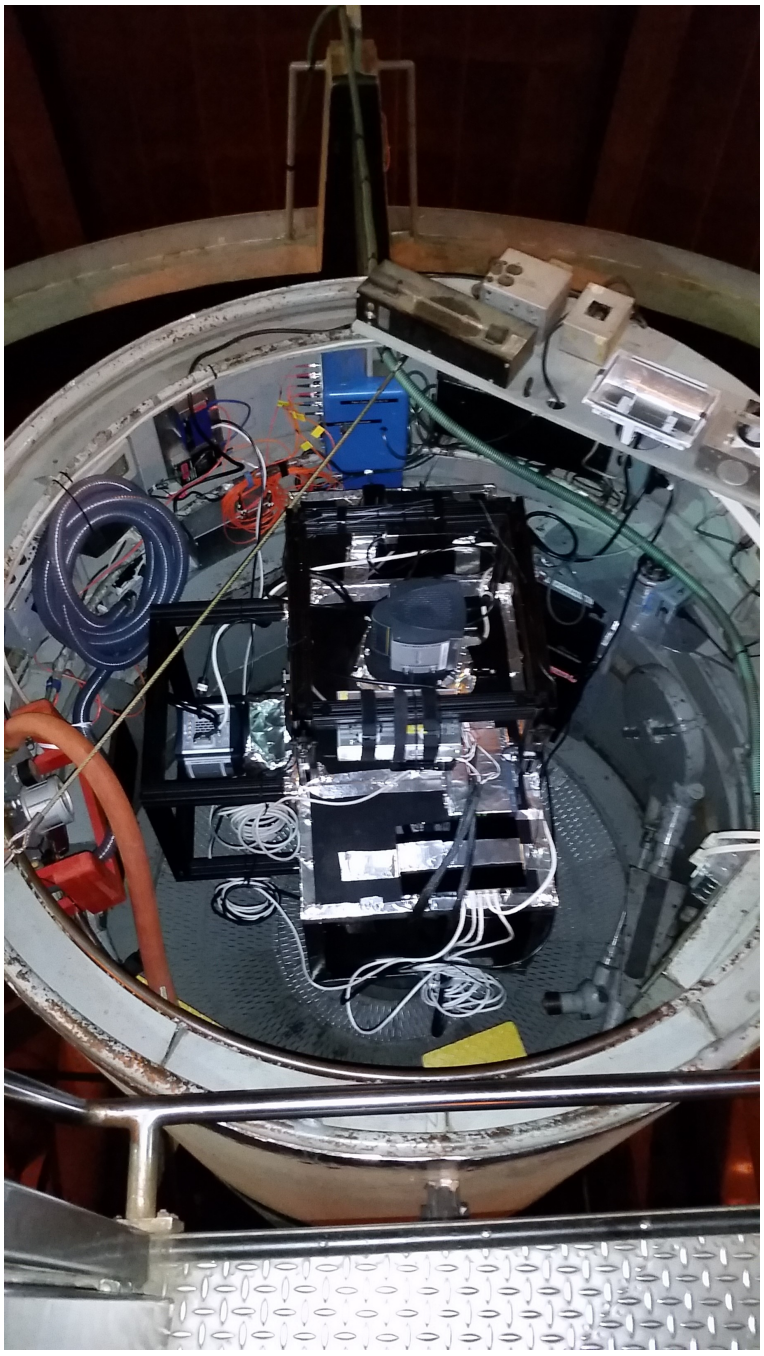

Figure 2-2: A picture of the CHIMERA at Palomar [3]. This instrument was used to obtain high speed images that served as the basis of my lightcurve modelling.

Chapter 3

HW Vir Class Binary Systems

An HW Vir class binary consists of a hot sub dwarf with a brown dwarf or main sequence star companion. There are ∼200 known (and candidate) HW Vir class binaries, making them relatively rare objects [8]. Although the exact physics underlying their formation remains an open problem, past studies suggest that they form through the process of the common envelope effect [8]. In this chapter, we will discuss the formation process of HW Vir type systems, notable characteristics of their lightcurves, and the motivation for studying them.

3.1 Formation of HW Vir Class Binaries

3.1.1 Common Envelope Effect

The common envelope effect (CEE) is a stage in binary evolution where for a short period of time, the two stars share an envelope. It occurs in binary systems where the two stars are relatively close together due to their short orbital period so that when one of the stars evolves off the main sequence, it comes into contact with the other star and engulfs it. There are two possible outcomes for when a binary system enters the CEE: envelope ejection which leaves behind a tight binary system, or the merger of the two stars. When an envelope ejection takes place, the two stars eventually separated and go back to being a detached binary without a shared envelope. Although this

process plays a crucial role in understanding the formation and evolution of certain types of binaries, like the HW Vir class binary systems, there is still a lot unknown about this process [9] (we will further discuss some of these open questions in Chapter 3.3).

For this project, I focused on searching for short-period systems (i.e., sub 80-minute period binaries). These systems are special since they are under the 80-minute period threshold, which indicates that no stars in the binary can be on the main sequence. This is because for a given orbital period of a binary system, there is a minimum allowed density for objects called the *Roche limit*. When an object with a density smaller than allowed enters a binary system with a period larger than it is able to support, the star is tidally disrupted and the binary system becomes unstable. The limiting period for a typical main sequence star density is 80 minutes. Therefore, for these ultra compact binary systems, we know that the hot sub-dwarfs must have a degenerate companion like a brown dwarf. These brown dwarf HW Vir type systems form when the brown dwarf survives the red giant evolution stage of its companion (sdB) [10]. In other words, these systems form when a binary undergoes the common envelope effect, and the brown dwarf companion is ejected from the shared envelope, returning the system to a detached binary.

3.2 Lightcurves of HW Vir Class Binaries

The lightcurves of HW Vir class binary systems have a few key characteristics. Later in Chapter 4, we will use these visible characteristics to filter out and search for them among a large data set of lightcurves. Figure 1-3 is the lightcurve of ZTFJ2203+4824, which I analyzed for my project.

ZTFJ2203+4824 is an eclipsing binary, which means that many of the characteristics of its lightcurve are closely related to the physical parameters of the system, as we discussed in Chapter 1.3. First, take note of the relative depths of the primary and secondary eclipses. For a binary of an sdB and a brown dwarf, we expect a large difference in the depth of the primary and the secondary eclipse, due to the large

difference in the luminosity of the two objects. Generally, the luminosity of a brown dwarf is less than 1% of a sdB, which means that it is common for the second eclipse to be barely noticeable. In addition, HW Vir class stars are known for their strong reflection effect [10]; this is apparent in the sinusoidal pattern pattern observed in the out-of-eclipse region of the lightcurve. Although subtle, recognizing this pattern plays an important role in selecting out lightcurves of HW Vir class binaries because this strong reflection effect is one of the main observable characteristics of this type of binary.

Above, were the two main characteristics that I used to select HW Vir class binary candidates in the initial search process.

3.3 Motivation for Further Study

There have only been a handful of studies on HW Vir class binary systems so far; however, they can provide a great deal of information that allows us to learn more about the common envelope effect. For example, in a recent study [8], they aimed to catalog a range of HW Vir type systems, studying their properties such as the distribution of periods, and the distribution of the masses of the companion brown dwarfs. They aimed to better understand the limits of the common envelope effect, by studying systems that underwent a common envelope event.

My project aimed to search for and model short-period systems that increase the known number of HW Vir class binaries near the period minimum of main sequence star binaries. These limiting cases allow us to explore physics such as the lower bound limit on the mass of a companion that is able to survive a CEE, the lower bound on the shortest period orbit binary which resulted from an envelope ejection, etc. Brown dwarfs HW Vir systems are ideal for this study because they have low mass companions and form sub-80 minute period binaries which push the limits of the known shortest period HW Vir class binaries – neither of which can be accomplished with a main sequence star companion.

Chapter 4

Searching for Binary Systems

The main goal of this project was to design a pipeline to search for eclipsing binary systems in large-scale time-domain datasets. Although there are many advanced methods that can be employed, such as machine learning algorithms, I chose to use a simpler method for filtering and mining for eclipsing binaries. One of the most straightforward methods to search for eclipsing binaries is to look for periodic behaviors in lightcurves. In this section, I will describe the tools that I used to perform the period search and the method of how I selected lightcurves for my analysis.

4.1 Periodicity of Lightcurves

As we briefly discussed in Chapter 1.3, one of the main characteristics of an eclipsing binary system's lightcurve is its periodic flux modulation. We can exploit this property to search for binary systems by searching for lightcurves exhibiting periodic behavior. We can do so by using various algorithms. For example, for continuously sampled data, we can perform a discrete Fourier transform. For randomly sampled data like those from ZTF, we must use tools that perform modified Fourier-transform-like algorithms. There are many useful tools on various platforms, and for my analysis, I choose to use a Python package that is commonly used throughout the astrophysics community: the *Lomb-Scargle Periodogram* from the astropy library [11] .

4.1.1 Lomb-Scargle Periodogram

In general, there are several different approaches that can be used to search for periodicity in a given dataset: Fourier methods, phase-folding methods, least squares methods, and the Bayesian approaches. Statisticians have developed a method that combines these mathematical ideas to create a better and more effective approach to this problem. The result of the combined method is the *Lomb-Scargle periodigram* [12]. This tool is commonly used by researchers in a broad range of fields, including astrophysics, where scientists are interested in looking for periodic behaviors in their datasets.

One of the easiest ways to implement this algorithm is by using the Lomb-Scargle Python package under the astropy library. This algorithm allows you to feed in any set of time-varying data and returns the result of the algorithm in the form of a power spectrum (intensity vs frequency). In other words, the power spectrum tells us how prominent each of the frequencies are in a given dataset, The astropy implementation of this algorithm allows you to make certain specifications such as minimum and maximum frequency for the period search, how precisely you want to test each of the frequencies (i.e., how fine the frequency grid of the power spectrum will be), etc. For a complete list of options and the documentation, refer to [11].

4.2 Selecting Lightcurves: Methods

In order to search the ZTF lightcurves for periodicity, first I applied the Lomb-Scargle algorithm to all of the publicly available ZTF lightcurves. Note that since ZTF is a non-uniformly sampled dataset, we do not need to account for the effects of the Nyquist frequency – which we would have to account for other dataset that are uniformly sampled, such as TESS [12]. After passing all of the data through the algorithm, I sorted the results by their significance. The significance of the results is given in terms of the false alarm probability – which tells us the probability of finding a peak of the same height or higher if the data purely consisted of Gaussian noise that does not have any periodic behaviors. In simpler terms, it is a quantitative

measure of how likely it is for the peak in the power spectrum to have resulted from an actual periodic behavior in the dataset. By sorting the lightcurves from most to least significant, it sorts the lightcurves from those which are more likely to be of eclipsing systems to those that are least likely. Although this is not a perfect method for finding all of the eclipsing systems, given that not all eclipsing binaries will yield high significance, there are also other sources of light besides binaries that can produce periodic effects leading to a mix of systems with high significant results. However, since I am only using this method to simply filter out interesting candidates, it is not necessary that the method is precise. It simply provides a systematic order in which I will look through the lightcurves so that the ones that are more likely to be of interest will be near the top of my search process.

Once the lightcurves were sorted by significance, I selected interesting candidate lightcurves by eye. Using what I know about the characteristics of HW Vir's lightcurves (see Chapter 3.2), I examined each of the lightcurves to pick out potential candidates. Here, I choose to specifically select ultra-compact binaries (i.e., systems with periods of less than 80 minutes) since the goal of this project was to model a system with a brown dwarf companion. As we discussed in Chapter 3.3, these ultra compact systems allow us to study a subset of binaries that were produced by the process of the CCE. Further, these subset of binaries have short periods and low mass companions that allows us to learn about the limiting cases for the CCE.

Below (see Figure 4-1) is the phase-folded lightcurve and the power spectrum of ZTFJ2203+4824. As you can see from the power spectrum, the most prominent frequency in the lightcurve was 18.5 cycles per day, which is equivalent to an orbital period of 0.0543 days or $\sim$78 minutes. I phase-folded the raw data from ZTF and produced a phase-folded lightcurve, which is shown in the bottom panel of Figure 4-1. As you can see, the lightcurve of this system has many of the characteristics of a typical HW Vir type system. For example, there are two minima that correspond to the primary and secondary eclipse; we see that the primary eclipse much more prominent than the secondary eclipse as we would expect for an HW Vir class binary with a brown dwarf companion. Further, we observe a slightly sinusoidal pattern in

the out-of-eclipse region, which again suggests that this system is a HW Vir type system.

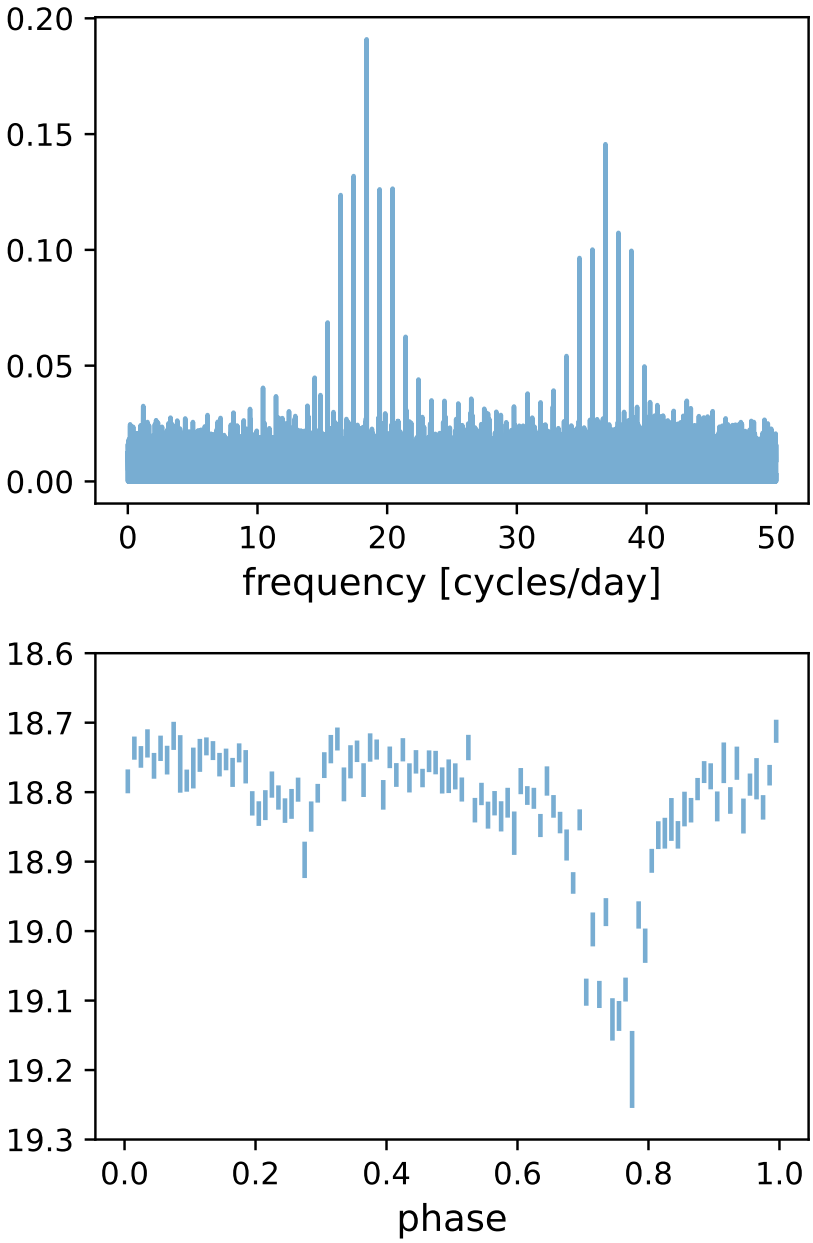

Figure 4-1: The power spectrum (top) and the phase-folded lightcurve (bottom) of a HW Vir class binary candidate I discovered from the initial sorting process using the Lomb-Scargle algorithm. As we see in the power spectrum, this system does not have one distinct peak but several peaks; this is because the lightcurve is not purely sinusoidal. A system would have one distinct peak only if the data was purely sinusoidal, but otherwise, the data is a sum of several frequencies, as we see in the above case. Taking the period of the above system to be given by the most prominent frequency we find in the power spectrum, it has a frequency of 18.5 cycles per day which is equivalent to a period of 0.0543 days or ∼78 minutes. Further, we can be confident that the above period is correct by taking a look at the phase-folded data which has the correct general shape of an eclipsing binary lightcurve.

Chapter 5

Modeling Lightcurves

The second goal of this project was to conduct a detailed study of one system of interest by modeling its lightcurve. In this chapter, we will discuss the lightcurve model I used for the analysis and the methods I employed in the fitting process.

5.1 The Model: ellc

One of the many tools developed for modeling lightcurves of eclipsing binary systems is called "ellc" [13]. The model requires a minimum input of at least four parameters for the eclipsing system (the radii of the objects, inclination, brightness ratio, and the time of superior conjunction, or mid-eclipse time); in addition, it can also account for approximately 40 other physical parameters of the system. Below are the nine parameters that I used to model the 78-minute period HW Vir type system I discovered. (For a description of other parameters refer to the model's documentation here: [13].)

There are a few parameters that I preset prior to the fitting process. The one parameter that I fixed in the modeling process was the **"period"**. I used the period for the binary determined by running the Lomb-Scargle algorithm on the ZTF data; I choose to do so because the ZTF data was sampled over the course of several years, whereas the lightcurve obtained from CHIMERA was taken over just 80 minutes, which makes the measurement of the period from ZTF data much more precise.

Another parameter that I choose to fix in my model is the **"shape"** of the stars. Because the objects in the binary are close to filling their Roche lobes, we expect each object to tidally deform. There, we want to treat each of the stars as a fluid object rather than a rigid spherical object. To do so, I fixed the shape of the star to be "roche" which then takes into account the deformation of the stars and the Roche lobe limit.

Here are now the parameters I fitted for. The first set of required parameters are **"radius_1"** and **"radius_2"** which are the radii of the two stars in the binary system, given in the units of the semi-major axis (i.e., r/a where r is the radius and a is the semi-major axis of the binary). The relative radii of each of the stars, as well as the semi-major axis play a role in determining the width of the eclipsing region of the lightcurve as well as its shape. Next is the **"sbratio"**– the surface brightness ratio of the two stars given as S_2/S_1, where S_1 and S_2 are the brightness of the stars 1 and 2, respectively. The ratio of the stars' luminosities plays a role in determining the absolute and relative depths of the primary and secondary eclipses. The model also requires the inclination **"incl"** which determines the shape of the bottom of the eclipses. Finally, the parameter **"t_zero"** is required, which specifies the time when the primary eclipse is at its minimum; this term does not provide any information about the physics of the system but is used to constrain the degree of freedom in the time axis.

For my analysis of the HW Vir system, I choose to fit the following extra physical parameters in addition to the required four. I chose these parameters based on known key features of an HW Vir type system. First is the mass ratio **"q"** of the two stars, where $q = m_2/m_1$ (m_1 is the mass of star 1 and m_2 is the mass of star 2). Although we cannot make measurements for each of the masses without the velocities of the objects from spectroscopic data, we are able to determine the relative masses of the two objects from the lightcurve. I also choose to fit for the **"heat_2"** parameter, which is a coefficient related to the reflection model of star 2. In my model, object 2 is the brown dwarf; I fitted for heat_2 because I expected some of the light from the hot sub dwarf to be reflected by the brown dwarf, which would yield a non-zero

reflection coefficient for star 2.

In addition to fitting for the above parameters from ellc, I also included a linear scaling term to account for any effects from normalization and changes in the flux intensity over time. For this, I multiplied the ellc lightcurve model by $(A + B(t - t_{mean}))$, where A and B are fit parameters, t is the time (i.e., the x-axis of the lightcurve), and t_{mean} is the mean time stamp of the data.

5.2 Fitting: Method

As one would expect, fitting a dataset to a function with 13 parameters is a challenging task. And due to the complexity of the functional form and the large number of parameters that are required for the fit, the simple chi-squared minimization method does not produce accurate results. To get a more precise fit and reliable uncertainties, a more advanced fitting method must be employed, such as the Monte Carlo Markov Chain (MCMC) method. For my analysis, I used a chi-squared minimization method as an initial fitting tool to obtain an approximate fit, then used the MCMC method for my final analysis to determine the values of the physical parameters and their uncertainties.

5.2.1 The Initial Fit

I first completed an initial fit using a minimization method to get rough estimates for each of the parameters. There are various Python packages that allow you to fit datasets to models using some form of minimization, but the basic idea is the same for all minimization methods. You take the residuals function (see Equation 5.1) and minimize that function for the data you are fitting for. The residuals are given as:

$$\left(\frac{y - y_{model}}{dy}\right)^2 \tag{5.1}$$

where y is the value of the data point, dy is the uncertainty on that point, and y_{model} is the predicted y value based on the model that you are testing.

5.2.2 The Monte Carlo Markov Chain (MCMC) Method

The Monte Carlo Markov Chain (MCMC) method is a more advanced method of fitting, which uses an algorithm that employs random sampling (i.e., a Monte Carlo) to determine a posterior distribution for each of the fit parameters.

In an MCMC, you provide a *prior*, then the algorithm takes random samples from these distributions. Any information that you have about the system is encoded into the priors so that it is accounted for in the MCMC sampling process; these priors for example include information about limits imposed on parameters due to physical limitations or based on estimations and prior knowledge about the system. After the specified number of samplings have taken place and the algorithm has converged, it creates a posterior distribution function (PDF). The PDF is the probability distribution that describes how likely each of the parameters will take certain values. Further, this distribution gives us the uncertainties for each fit parameter.

5.3 Modelling of ZTFJ2203+4824's lightcurve

Using the above ellc model and the two fitting methods, I fitted the g and r band lightcurves that were collected by the CHIMERA for ZTFJ2203+4824.

5.3.1 The Initial Fit

First, I fitted the lightcurve using a simple minimization method (method outlined in Chapter 5.2). Since I simultaneously fitted two lightcurves, I had to account for parameters that could be simultaneously fitted and others which had to be independently fitted since they differed for each color band. The independent parameters are: A and B terms for the linear offset, the brightness ratio, and the reflection coefficient. The linear offset term is simply a normalization term so by definition, it is independent for the two filters. The brightness ratio and the reflection coefficient depend on the wavelength of the emitted light; therefore, they also are independent for each of the filters. All of the other physical parameters that I fitted for are independent of

the wavelength so I fitted the same value to both the g and r band.

The final list of parameters that I fitted for are: the amplitude coefficient for the g and r bands, the time of the primary eclipse, the radii of each of the stars, inclination, brightness ratio, the mass ratio, and the reflection coefficient of the brown dwarf. To account for the simultaneous fitting of both sets of data, I used a modified residual equation:

$$\left(\frac{y_r - y_{model}}{dy_r} + \frac{y_g - y_{model}}{dy_g}\right)^2 \tag{5.2}$$

where y_r and dy_r are the flux and uncertainty of flux for the r band data and y_g and dy_g are the flux and uncertainty of flux for the g band data. Figure 5-1 is the plot of the fit over the CHIMERA data. Further, see Table 5.3.2 for the values of each of the parameters of the lightcurve.

parameter	value [units]
A_{g}	0.16
A_{r}	0.63
B_{g}	0.0064
B_{r}	0.015
period	0.054 days
radius 1 (r_1/a)	0.23
radius 2 (r_2/a)	0.11
t_zero	59873 days
inclination	89.9 degrees
brightness ratio (g band)	0.00010
brightness ratio (r band)	0.00010
mass ratio	0.99
heat_2 (g band)	4.1
heat_2 (g band)	0.63

Table 5.1: Value of the fit parameters from fit using the simple residual minimization method. Note that the period was fixed (i.e., was not treated as a free parameter in the fitting process) based on the previous period that was determined from a period searching algorithm. There are no uncertainties reported here since we canot get accurate values for those with this method.

5.3.2 MCMC Fit

To obtain more reliable estimates of these values and their uncertainties, I repeated the same fitting process with the Monte Carlo Markov Chain (MCMC) method. As discussed in Chapter 5.2.2, I provided a prior for each of the fit parameters. For all priors except for the inclination, I used a uniform distribution. I selected the range of each of the parameters based on the physical limitations of the system and choose reasonable ranges for each parameter based on what was determined by the initial fitting process. Priors for r_1 and r_2 were determined by the physical limits of the stars' radii. I set the sampling range to $0.1 \sim 0.5$. I also imposed a Roche lobe overflow limit to prevent any errors that may occur in the ellc model caused by an overflow. The maximum size of a Roche lobe for each object in a binary system is given as a function of the mass ratio of each of the stars:

$$\frac{R_2}{a} = \frac{0.49q^{2/3}}{0.6q^{2/3} + \ln(1 + q^{1/3})}, \tag{5.3}$$

where R_2 is the radius of object 2, a is the semi-major axis of the binary system, and q is the mass ratio given as m_2/m_1. Next, since the brightness ratio is given as S_2/S_1 and I expect the hot subdwarf to be much more luminous, I expected the ratio to be much smaller than 1. To avoid fitting for small values, I fitted for the brightness ratio as (1/sbratio) with a range of $1 \sim 10000$. Similarly, the mass ratio q can be estimated according to the known masses of brown dwarfs and the hot sub dwarfs; using those values, I selected the prior to be $0.1 \sim 10$. The prior for the reflection coefficient was chosen to range from $0 \sim 10$ based on estimations from the initial fit for the coefficient. Lastly, unlike the other parameters, I did not use a uniform sampling for the prior of the inclination and instead used a cosine distribution with the inclination angle ranging from $0 \sim 90$ degrees. I choose this distribution because due to the geometry of the system, the cosine function best describes the probability distribution for inclinations of binary systems.

The corner plot produced by the MCMC fit is given below in Figure 5-2, and Figure 5-3 gives the plot of the final fit to the lightcurve. Further, see Table 5.3.2

for a list of the final fit parameters and uncertainties produced by the MCMC fitting method.

parameter	value ± uncertainty
A_{g}	0.15864 ± 0.00060
A_{r}	0.6473 ± 0.0027
B_{g}	-0.002 ± 0.012
B_{r}	-0.247 ± 0.075
period	0.054 days
radius 1 (r_1/a)	0.3459 ± 0.0071
radius 2 (r_2/a)	0.1661 ± 0.0075
t_zero	59873.123128 ± 0.000035
inclination	0.178 ± 0.0025
1/brightness ratio (g band)	5264 ± 2789
1/brightness ratio (r band)	4883 ± 2953
mass ratio	3.37 ± 0.74
heat_2 (g band)	1.44 ± 0.14
heat_2 (r band)	0.86 ± 0.14

Table 5.2: Above is a table with the results of the MCMC fitting process. The values of the fit parameters and their uncertainties are as given above. See Figure 5-2 for the corner plot that produced these results, and see Figure 5-3 for the plot of the fitted model over the raw data.

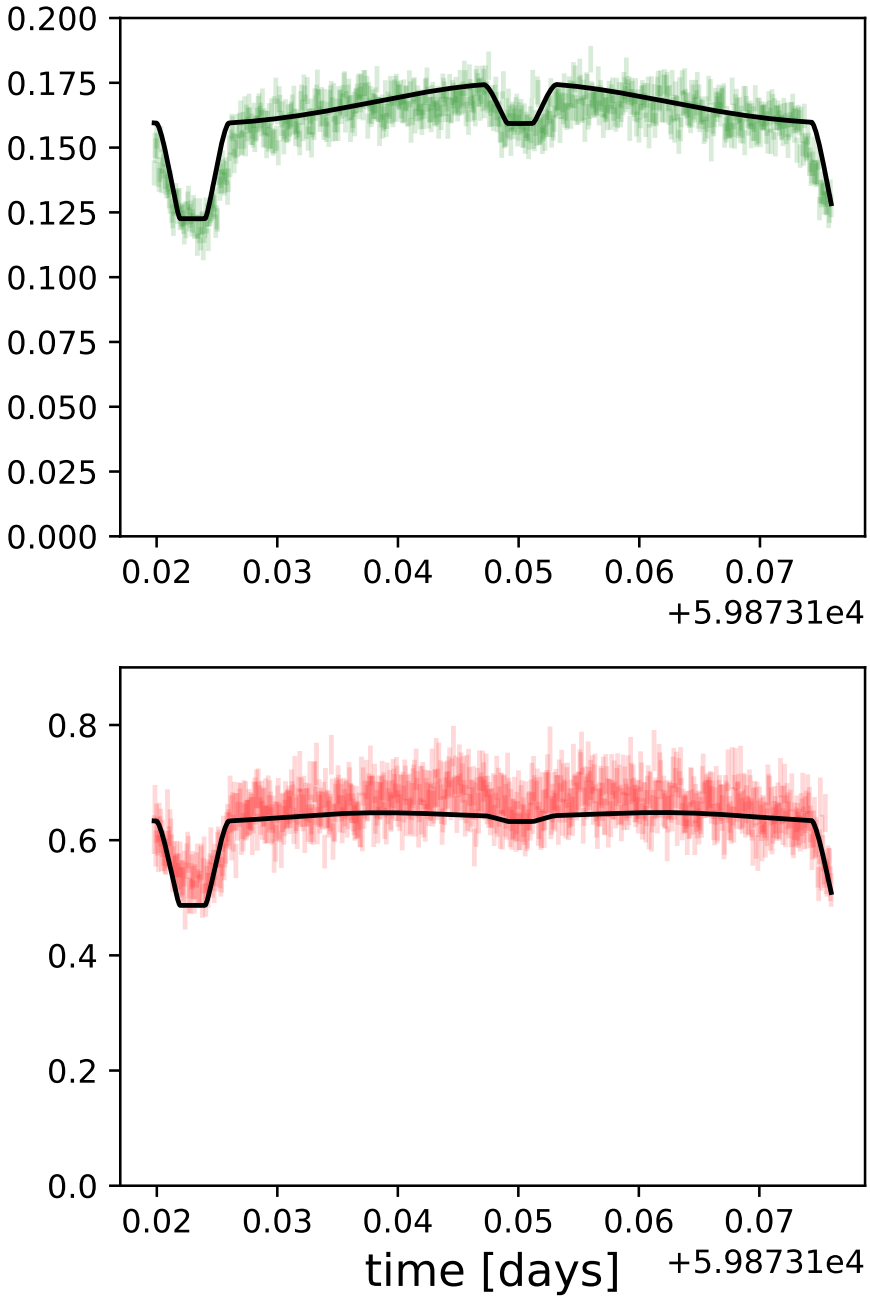

Figure 5-1: Initial fit using the residual minimization method for the r and g band data for ZTFJ2203+4824 collected by CHIMERA. The top plot is the g band and the bottom plot is the r band fit. The green and red uncertainty bars represent the uncertainty of the data and the black line is the fit to the data. As we see, it is a relatively good fit, but a better fit can be obtained with other methods such as the MCMC method.

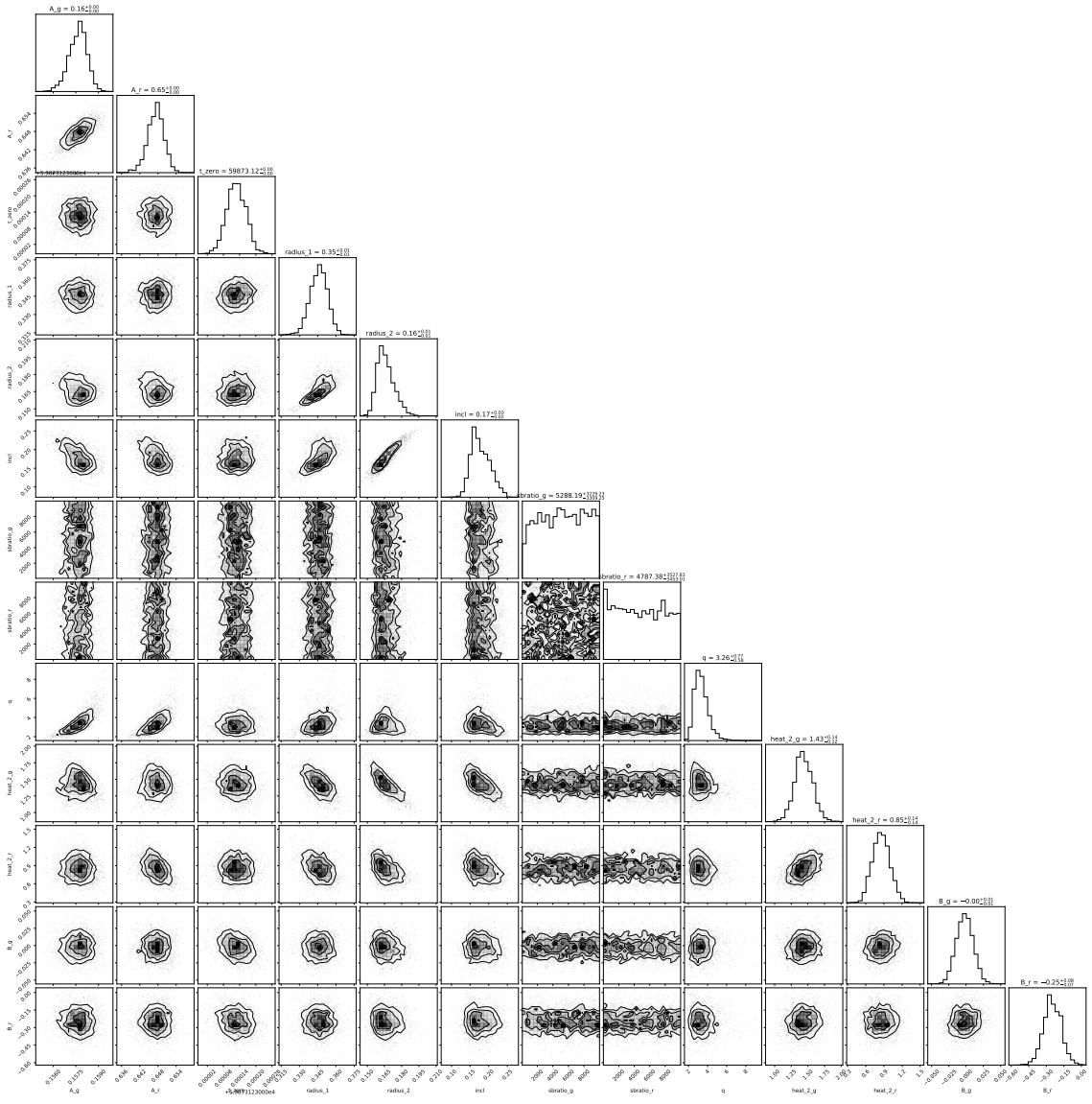

Figure 5-2: The corner plot produced by the MCMC algorithm. As we can see from the histograms, most of the posterior distributions take a Gaussian form; this shows that I sampled a good range for each of the parameters and that they converged on reasonable values. The two distributions that do not take a Gaussian form are for the brightness ratios, which tells us that the model is not as sensitive to those values. Additionally, we find that the majority of the parameters are not correlated, as we would expect. The only correlation is observed when comparing the same physical parameters across the two bands (e.g., the brightness ratio for the g and r band). This is expected since although the magnitudes of these values may differ based on the wavelength, they are still fundamentally measuring the same physical properties of the system.

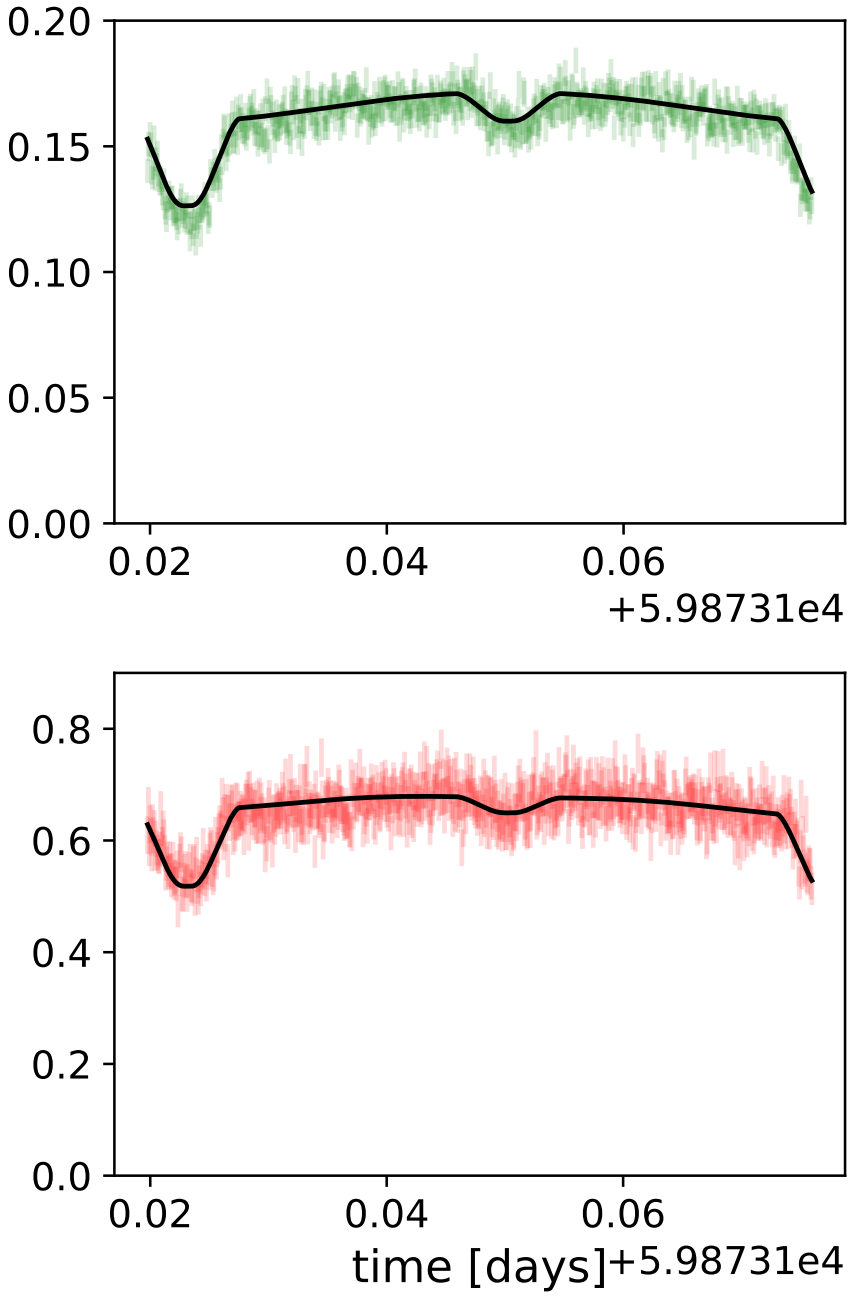

Figure 5-3: The result of the fit using the MCMC modeling method. The top plot is the g band and the bottom plot is the r band fit. The green and red uncertainty bars represent the uncertainty of the data and the black line is the fit to the data. The red and the green show the flux and the uncertainties collected by the CHIMERA telescope for the r and g band respectively, for ZTFJ2203+4824.

Chapter 6

Conclusion and Discussion

6.1 Discussion of the Results

The goal of this project was to design a systematic method to search for eclipsing binary systems from large datasets, and to further investigate an interesting binary system by modeling its lightcurve. Overall, these goals were met and I successfully discovered and measured the physical parameters of an eclipsing binary system. In Chapter 4, I discussed the binary search method that I used for this project and I introduced ZTFJ2203+4824, a 78-minute period HW Vir class binary system that I discovered. Further, in Chapter 5, I modeled its lightcurve using the MCMC modeling method to determine several physical parameters and their uncertainties for ZTFJ2203+4824.

Through the fitting process, I measured the radius of the two objects to be $r_{sdB} = (0.3459 \pm 0.0071)a$ and $r_{BD} = (0.1661 \pm 0.0075)a$, where a is the semi-major axis of the binary. To get the actual values of the radii, we need to know the semi-major axis a for the system, which we cannot determine since we do not know the orbital velocities of the system. Therefore, we will take the typical masses of the a brown dwarf and a sdB to estimate the typical semi-major axis of a HW Vir type system to continue with our analysis. Kepler's third law gives us the relation between the

period, semi-major axis, and the total mass of the system:

$$\frac{a^3}{T^2} = \frac{G(M_{\rm sdB} + M_{\rm BD})}{4\pi^2}, \tag{6.1}$$

where a is the semi-major axis, T is the period, G is the gravitational constant, and M_{sdB} and M_{BD} are the masses of the sdB and the brown dwarf, respectively. With the above relation, using the typical masses of sdBs ($M_{sdB} = 0.47$ solar masses) and brown dwarfs ($M_{BD} = 0.06$ solar masses), we estimate the semi-major axis of the system to be $a = 0.488$ solar radii. Further, with this estimated value of a we can determine the radii of the two stars: $r_{sdB} = (0.1689 \pm 0.0034)$ solar radii and $r_{BD} = (0.0811 \pm 0.0037)$ solar radii. sdBs typically have a radius of $0.15 \sim 0.25$ solar radii, and the radius of a brown dwarf typically ranges from $0.066 \sim 0.12$ solar radii [14], which is in agreement with the measured radii of the system. In addition, we find that the brightness ratio of the two stars is also in agreement with the typical luminosities of sdB and brown dwarfs. The brightness ratio (given as S_{sdB}/S_{BD}) was measured to be 5264 ± 2789 and 4883 ± 2953 for the g and r band respectively. Given that the luminosity of a brown dwarf is negligible compared to that of an sdB, the order of magnitude of 10^3 for the brightness ratio is reasonable. Lastly, through the fitting process, the mass ratio (given as m_{sdB}/m_{BD}) was measured to be 3.37 ± 0.74. Again, this value is in agreement with the typical masses for the two stars in this system.

All of these measured physical parameters are in agreement with an HW Vir type system comprised of a hot sub-dwarf and a brown dwarf, as I predicted from the ZTF lightcurve. Now with a confirmation of what type of system this binary is based on the measured physical parameters, this HW Vir class binary can be used for further investigations – such as population studies of HW Vir class systems and the common envelope effect.

6.2 Areas for Further Research

One way to improve this analysis would be to collect spectroscopic data for this system. Although I was not able to obtain spectroscopic data for this target (due to poor weather and target visibility), if additional data were to be collected, it would allow for the measurement of radial velocities. This would be done using the following relation known as the Doppler shift:

$$\frac{\lambda_r}{\lambda_s} = \frac{f_s}{f_r} = \sqrt{\frac{1+\beta}{1-\beta}}, \tag{6.2}$$

where λ_r and λ_s are the wavelengths measured by the receiver (i.e., telescope) and sender (i.e., the star), respectively; f_r and f_s are the frequencies measured by the receiver and the sender; and finally, $\beta = v/c$, where v is the relative velocity between the sender and the receiver and c is the speed of light. Knowing the transnational velocity allows us to measure the semi-major axis of the system, which in turn also allows us to determine the masses for each of the objects (i.e., beyond the mass ratio we currently have) and the radii of each of the objects (i.e., not as a ratio in terms of the semi-major axis).

Another avenue for further research would be to improve the data mining method to create a larger population of HW Vir candidates. This would allow for population studies which would provide insight into the process of the common envelope effect. The distribution of periods and the distribution of masses of the companion would allow us to better understand what low-end constraints might exist on what types of objects are able to survive the common envelope effect and produce a hot subdwarf.

6.3 Broader Impacts

The study of ultra-compact binaries such as ZTFJ2203+4824, is also of great interest in the field of gravitational wave astrophysics. In recent years, there has been a growth of interest in these systems among the gravitational-wave astrophysics community because of their detectability by gravitational waves. During their orbits, due

to the tidal effects, the system can lose energy. This energy is lost in the form of gravitational waves and allows physicists to detect them on instrumentation, such as the Laser Interferometer Gravitational-Wave Observatory (LIGO) [15] and the Laser Interferometer Space Antenna (LISA) [16]. The data from gravitational waves not only allows researchers to detect these systems but can also provide valuable information about the evolution of the system and interesting astrophysical phenomena.

Bibliography

[1] Harvard-Smithsonian Center for Astrophysics. Pulsating variable stars and the hertzsprung-russell (h-r) diagram. URL `https://chandra.harvard.edu/edu/formal/variable_stars/bg_info.html`. Last accessed 11 February 2023.

[2] Zwicky transient facility (2022). URL `https://www.ztf.caltech.edu/multimedia.html`. Last accessed 11 November 2022.

[3] Caltech high-speed multi-color camera: a prime focus instrument for the palomar 200-inch (2014). URL `http://www.tauceti.caltech.edu/chimera/`. Last accessed 15 February 2023.

[4] Burdge, K. B. *et al.* A dense 0.1-solar-mass star in a 51-minute-orbital-period eclipsing binary. *Nature* **610**, 467–471 (2022). URL

[5] Ricker, G. R. *et al.* Transiting Exoplanet Survey Satellite (TESS). *Journal of Astronomical Telescopes, Instruments, and Systems* **1**, 014003 (2015).

[6] Bellm, E. C. *et al.* The Zwicky Transient Facility: System Overview, Performance, and First Results. *Pub. Ast. Soc. Pac.* **131**, 018002 (2019). `1902.01932`.

[7] Harding, L. K. *et al.* CHIMERA: a wide-field, multi-colour, high-speed photometer at the prime focus of the hale telescope. *Monthly Notices of the Royal Astronomical Society* **457**, 3036–3049 (2016). URL

[8] Schaffenroth, V. *et al.* The EREBOS project: Investigating the effect of substellar and low-mass stellar companions on late stellar evolution. Survey, target selection, and atmospheric parameters. *Astron. Astrophys.* **630**, A80 (2019). `1907.09892`.

[9] Ivanova, N. *et al.* Common envelope evolution: where we stand and how we can move forward. *The Astronomy and Astrophysics Review* **21** (2013). URL

[10] Heber, U. Hot subluminous stars. *Publications of the Astronomical Society of the Pacific* **128**, 082001 (2016). URL

[11] Lomb-scargle periodograms (2023). URL https://docs.astropy.org/en/stable/timeseries/lombscargle.html. Last accessed 16 February 2023.

[12] VanderPlas, J. T. Understanding the Lomb-Scargle Periodogram. *Astrophys. J. Supp.* **236**, 16 (2018). 1703.09824.

[13] Maxted, P. F. L. ellc: A fast, flexible light curve model for detached eclipsing binary stars and transiting exoplanets. *Astron. Astrophys.* **591**, A111 (2016). 1603.08484.

[14] Sorahana, S., Yamamura, I. & Murakami, H. ON THE RADII OF BROWN DWARFS MEASURED WITHiAKARI/iNEAR-INFRARED SPECTROSCOPY. *The Astrophysical Journal* **767**, 77 (2013). URL

[15] Abramovici, A. *et al.* LIGO: The Laser Interferometer Gravitational-Wave Observatory. *Science* **256**, 325–333 (1992).

[16] Amaro-Seoane, P. *et al.* Laser Interferometer Space Antenna. *arXiv e-prints* arXiv:1702.00786 (2017). 1702.00786.